Journal of Alloys and Compounds 541 (2012) 483–487

Contents lists available at SciVerse ScienceDirect

Journal of Alloys and Compounds

journal homepage: www.elsevier.com/locate/jalcom

Fabrication and temperature-dependent magnetic properties of one-dimensional embedded nickel segment in gold nanowires

S. Ishrat [a], K. Maaz [a,c], Kyu Joon Lee [b], Myung-Hwa Jung [b], Gil-Ho Kim [a,*]

[a] School of Electronic and Electrical Engineering and Sungkyunkwan Advanced Institute of Nanotechnology (SAINT), Sungkyunkwan University, Suwon 440-746, Republic of Korea
[b] Department of Physics, Sogang University, Seoul 121-742, Republic of Korea
[c] Nanomaterials Research Group, Physics Division, PINSTECH, Nilore, Islamabad, Pakistan

ARTICLE INFO

Article history:
Received 16 April 2012
Accepted 28 June 2012
Available online 6 July 2012

Keywords:
Nanostructured materials
Anisotropy
Magnetic measurements

ABSTRACT

In this paper, we elucidate the fabrication and temperature-dependent magnetic characteristics of Ni nanowires sandwiched in Au nanosegments. The nanowires were fabricated by electrochemical deposition in alumina templates with diameter of 100 nm and Ni segment length of around 800 nm. Structural analyses confirmed the formation of pure phase, crystalline multi-segmented Au–Ni–Au nanowires. Magnetic studies performed using a super-conducting quantum interface device-vibrating sample magnetometer reveal that ferromagnetism is induced in the wires due to the presence of Ni, which is ferromagnetic in nature. Temperature-dependent analysis shows that coercivity of the samples increases with decreasing temperature following Kneller's law for ferromagnetic nanostructures. The saturation magnetization shows an increasing trend as the temperature decreases according to the modified Bloch's law and this behavior is similar to that of ferromagnetic nanoparticles.

1. Introduction

In the past decade, nanostructured materials have attracted considerable attention owing to their potential applications in both the investigation of mesoscopic physics and fabrication of nanodevices. One-dimensional magnetic nanowires have been extensively used for magnetic recording and spintronic applications [1,2]. These materials are very promising candidates for a variety of applications in electronics, medical industries, and in high-density magnetic storage devices [3–5]. Arrays of magnetic nanowires can be produced by different techniques and, among these techniques, electrochemical deposition is very common and easily achievable at room temperature [3]. From the processing point of view, electrochemical deposition is one of the most favorable techniques for the fabrication of template-assisted nanowires and is accomplished by depositing their ions into the pores of the host membranes [6,7]. Highly ordered nanoporous alumina has been used as the hosting material to grow the nanowires reported here. Compared to single segment nanowires, multi-segment nanowires offer more diverse functionality if their morphology is carefully controlled during fabrication. Composition-modulated nanowires have been frequently reported, whereas diameter-modulated nanowires consisting of a bead-like structure have been rarely reported in literature [8,9].

Magnetic characterization of highly ordered arrays of ferromagnetic nanowires is of growing interest for their application as the spintronic materials. The intrinsic nature of these nanowires consists of nanomagnets give rise to the interesting magnetic properties at room temperature and at lower temperatures that are different from their bulk counterparts. Arrays of segmented nanowires with diameter of few hundred nanometers and length of few microns are suitable candidates for a variety of applications in recent technology [3]. When the temperature of the system is decreased below room temperature, the thermal energy ($E_{th} = K_BT$) is suppressed by the anisotropy energy ($E_a = K_{eff}V$) of the system that enhances the magnetic order of the system. At low temperature, the simple thermal activation model, where the particle's moment over the anisotropy barrier is suppressed, is applicable. In this situation, at low temperatures, the material follows *Kneller's law* for ferromagnetic nanoparticles in the temperature range (0–T_B), where T_B is the superparamagnetic blocking temperature of the system, while the saturation magnetization follows the modified *Bloch's law* similar to the case of ferromagnetic nanoparticles [10].

In this work, segmented Au–Ni–Au nanowires have been fabricated by electrochemical deposition; structural characterization was done by scanning electron microscopy (SEM), transmission electron microscopy (TEM), and X-ray diffraction (XRD) techniques while magnetic characterization was done by a super-conducting quantum interface device–vibrating sample magnetometer (SQUID–VSM) in the temperature range 300 to 2 K. For magnetization analysis, the wires were left embedded in anodized aluminum oxide (AAO)

* Corresponding author. Tel.: +82 31 290 7970; fax: +82 31 299 4618.
E-mail address: ghkim@skku.edu (G.-H. Kim).

0925-8388/$ - see front matter © 2012 Elsevier B.V. All rights reserved.
http://dx.doi.org/10.1016/j.jallcom.2012.06.136

templates while they were liberated from the templates for structural analysis.

2. Material and methods

In electrochemical deposition, there are different modes of deposition such as constant current pulses, constant voltage pulses, and by alternating pulses. In the present work, the Au–Ni–Au nanowires were electrochemically deposited by constant voltage pulses. We fabricated Au–Ni–Au nanowires by electrochemical deposition in porous AAO templates that were used as scaffold templates with a pore diameter of 100 nm and thickness of about 13 mm. To grow the multi-segment nanowires, one side of the AAO template was used as a cathode surface. In order to make one side conductive, a thin silver (Ag) layer of ~2 μm thickness was evaporated by an electron beam (EBM) evaporator. A three-electrode DC cell was used for the deposition process, where Ag/AgCl was used as the reference electrode, platinum as the counter electrode, and AAO with a backside Ag layer as the working electrode. A thin sacrificial Ag layer of ~2 μm was electrodeposited for uniformity of the cathode surface. Gold plating solution was used for the deposition of Au segments while Ni sulfate solution was used for the growth of the Ni segment.

The as fabricated nanowires were electrodeposited by applying a constant DC voltage (−0.95 V) and the length of the nanowires was tuned by controlling the deposition time and quantity of deposited charges during the fabrication process. The Au segment length was fixed at both ends up to 1 μm and the Ni segment length was controlled up to 800 nm. After deposition, the template was kept in nitric acid for 15 min to remove the Ag layer used prior to the deposition, and later the template was dissolved in 3 M NaOH solution for 45 min. To remove NaOH from the wires, the samples were washed with deionized water by centrifugation. After cleaning, the nanowires were dispersed on a silicon wafer and dried at 120 °C for 20 min for the structural analysis. Further details of fabrication are given in our previous work [11]. Structural characterization was performed by XRD, SEM, and TEM. Energy dispersive spectroscopy (EDX) was used to determine the average chemical composition of the nanowires. Magnetic hysteresis loops were taken by SQUID–VSM under a constant applied field and by varying the sample temperature from 300 to 2 K.

3. Results and discussion

The scanning electron microscope images of the wires with nickel segment length of 800 nm, which is sandwiched between the two Au segments, are shown in Fig. 1(a and b). The TEM analysis of the same Ni segment is presented in Fig. 1(c), and it shows that the Ni segment is composed of nanoparticles of approximately 100 nm diameter aligned in one direction to form the nanowires. In Fig. 1(b and c), the non-uniformity in diameter of the Ni segment can be seen, and it varies from 90 to 110 nm. This might be due to the particle size distribution constituting the nanowires. The selective area electron diffraction (SAED) pattern of Ni segment obtained from HRTEM (using FFT) is shown in Fig. 1(d). This analysis confirms the polycrystalline nature of the Ni segment. Fig. 2(a) shows the X-ray diffraction pattern of the prepared nanowires in which the observed peaks are indexed according to the standard PCPDF cards for Ni and Au, with additional silicon and oxygen peaks appearing from the substrate material. There seems to be no impurity peaks in the XRD pattern, thus confirming that the nanowires are of pure phase. The EDX pattern of the nanowires shown in Fig. 2(b) reveals the presence of Au and Ni in the wires with Si and O peaks coming from the Si/SiO_2 substrate. The results of XRD and EDX confirm that the as-fabricated nanowires are of pure phase and purely crystalline in nature.

For magnetic analysis, the magnetization loops $M(H)$ were recorded at different temperatures from 2 to 300 K under an applied field of 4 kOe as shown in Fig. 3(a–f). In these measurements, the field is applied parallel to the wire length expecting that the direction of anisotropy is along the wire's length. From our previous work [11], it is known that ferromagnetism in such nanowires arises because of the Ni embedded between the two Au segments. The coercivity (H_c) values as deducted from the $M(H)$ loops at different temperatures are plotted in Fig. 4(a) where it is seen that H_c increases as the temperature decreases from 300 to 2 K. At low temperatures, below 20 K, there seems to be saturation in H_c values as the temperature goes down to 2 K. To interpret our results, we consider that our nanowires are composed of beads (i.e., nanoparticles of about 100 nm diameter) as shown in the TEM image

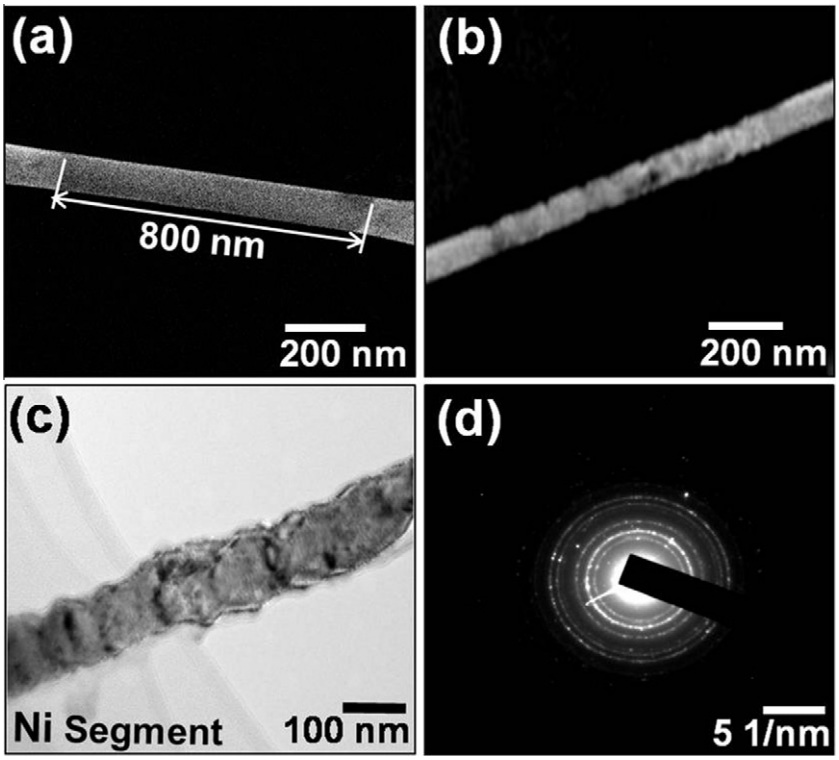

Fig. 1. (a) SEM image of Au–Ni–Au nanowire with 800 nm Ni segment length and 100 nm wire diameter, (b) SEM image of Ni segment sandwiched between two Au segments, (c) TEM image of Ni segment showing bead-like structure and (d) SAED pattern of Ni segment showing the polycrystalline nature of the wires.

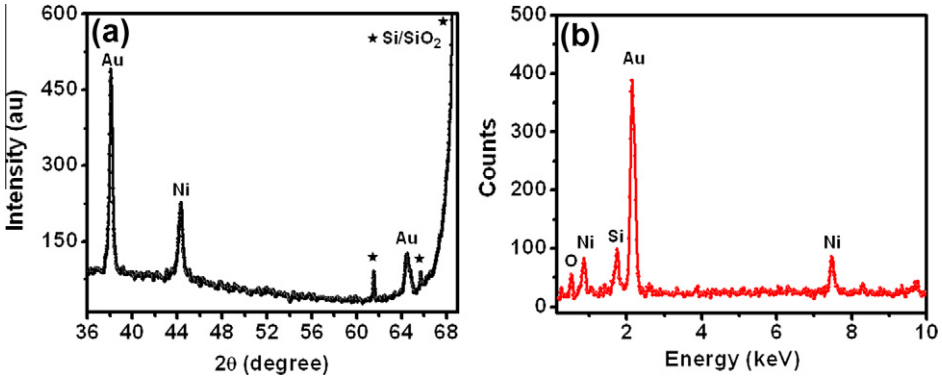

Fig. 2. (a) XRD pattern of wires confirms crystalline nature of nanowires composed of Ni and Au and (b) EDX analysis showing the composition of nanowires with visible Au and Ni peaks.

(Fig. 1(c)) as discussed earlier. It is understandable that metallic Ni nanoparticles are aligned in one dimension constituting segmented nanowires. Thus, under these circumstances, the simple model of thermal activation of particles moment over the anisotropy energy barrier is applicable to these segmented nanowires in the temperature range 300 to 2 K. According to Kneller's law

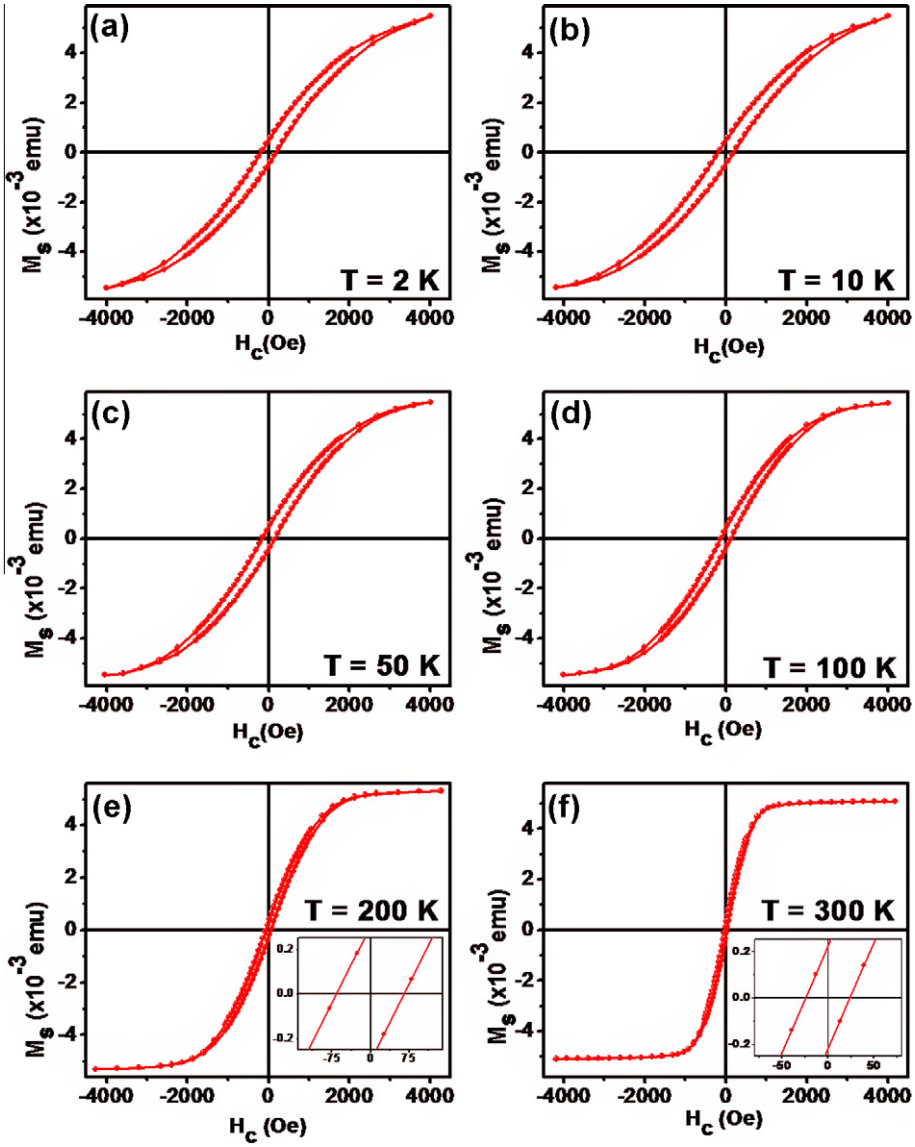

Fig. 3. Magnetization hysteresis loops $M(H)$ of wires embedded in AAO templates taken at temperatures: (a) 2 K, (b) 10 K, (c) 50 K, (d) 100 K, (e) 200 K, and (f) 300 K under an applied field of 4 kOe. Inset (e) shows hysteresis loop at 200 K enlarged at 140 kOe and (f) shows hysteresis loop at 300 K enlarged at 80 kOe.

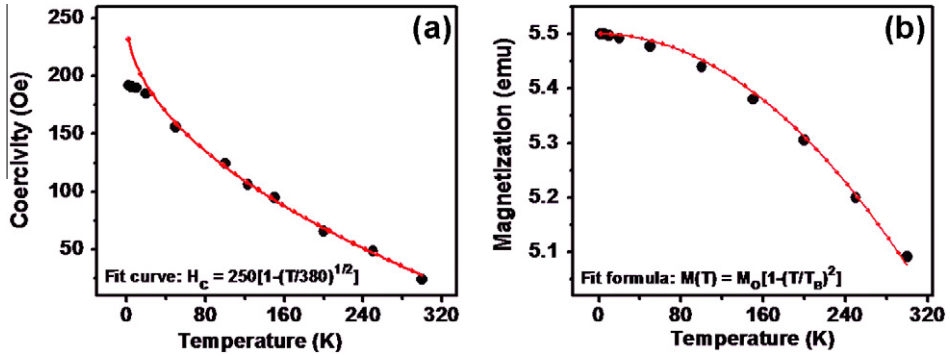

Fig. 4. Plot of (a) coercivity as a function of temperature following Kneller's law shown by red line in graph (b) magnetization as a function of temperature in the range (2 to 300 K). Red line represents the theoretical modified Bloch's law followed by the experimental data. (For interpretation of the references to color in this figure legend, the reader is referred to the web version of this article.)

for ferromagnetic nanoparticles, the coercivity (H_c) in the temperature range (0–T_B) can be written in the form based on the simple model [12,13]:

$$H_c = H_o[(1 - T/T_B)^{1/2}] \quad (1)$$

where H_o is the coercivity at 0 K that can be obtained by extrapolating the H_C versus T curve to the field axis, and T_B is the superparamagnetic blocking temperature of the nanoparticles. Referring back to Fig. 4(a), the red line shows the fit curve according to Kneller's law using T_B as the fitting parameter. It is evident in the figure that the experimental data fits very well to the above relation in the high temperature region (300 to 20 K). However, below 20 K the data shows some deviation from the fit curve. Thus, this law (Kneller's) appears to be applicable in the temperature range 300 to 20 K, while below 20 K this model is not valid for our system. The deviation of H_C from Kneller's law at low temperatures could be due to the freezing spin effects in the nanowires this gives no response to the applied field resulting in the saturation of H_C values of the samples. Similar effects have been observed by O. Iglesias et al. [14] based on the Monte Carlo simulation of the coercivity dependence on the temperature of γ-Fe_3O_4 spherical nanoparticles.

The magnetization measurements at different temperatures (300, 250, 200, 150, 100, 50, 20, 10, 5, and 2 K) for the nanowires are presented in Fig. 4(b). From the figure, it is seen that the saturation magnetization (M_S) increases with decreasing temperature of the samples. In the case of Bloch's law for bulk ferromagnetic systems, the saturation magnetization below the Curie temperature is expressed as [15].

$$M(T) = M(0)[1 - (BT)^{\alpha}] \quad (2)$$

where B is Bloch's constant and depends on the nature of the materials, and α is Bloch's exponent with a value of 3/2. This law is generally valid for bulk materials in the high temperature range. However, in case of nanostructured materials, due the finite size effects the thermal dependence of magnetization, the saturation magnetization deviates from the normal Bloch's law as the magnons with wavelength larger than the material's dimensions cannot be excited, and a threshold of thermal energy is required to generate spin waves in the materials. Thus, in the case of nanoparticles, the spin wave structure is modified in the form of a power law (T^{α}) with Bloch's exponent larger than its bulk value ($\alpha = 2$). Thus, in nanostructured materials, Bloch's law is modified to the form [16–18]:

$$M(T) = M(0)[1 - (BT)^2]. \quad (3)$$

This is known as the modified Bloch's law. In this case, Bloch's constant (B) is the reciprocal of the blocking temperature (T_B) of the nanomaterial ($B = 1/T_B$). The value of α in the modified Bloch's law has been experimentally determined by C.R. Alves et al. [17]. They have observed that for a large $CuFe_2O_4$ nanoparticles, the value of α was 1.5 whereas for smaller particles this value was close to 2. The difference in the values of α has been attributed to the finite size effects of nanostructured materials. Referring back to our results shown in Fig. 4(b) discussed earlier, the nanowires are composed of nanoparticles shown in Fig. 1(c); we observed that the modified Bloch's law with $\alpha = 2$, shown by the red line in Fig. 4(b), is fully satisfied for our nanowires in the temperature range (2 to 300 K). Therefore, we conclude that our system of segmented nanowires follows the modified Block's law for ferromagnetic materials.

4. Conclusion

Au–Ni–Au nanowires were fabricated by electrochemical deposition in alumina templates with diameter of 100 nm and Ni segment length of around 800 nm. Structural analyses confirmed the formation of pure phase, crystalline nanowires. Coercivity was found to increase with decreasing temperature, following Kneller's law for ferromagnetic nanostructures. The saturation magnetization showed an increasing trend as the temperature decreased according to the modified Bloch's law, which has been attributed to the finite size effects in segmented nanowires.

Acknowledgments

This research was supported by the World Class University program funded by the Ministry of Education, Science and Technology through the National Research Foundation of Korea (R32-10204).

References

[1] T.T. Albrecht, J. Schotter, G.A. Kastle, N. Emley, T. Shibauchi, L.K. Elbaum, K. Guarini, C.T. Black, M.T. Tuominen, T.P. Russell, Science 290 (2000) 2126.
[2] T. Nautiyal, T.H. Rho, K.S. Kim, Phys. Rev. B 69 (2004) 193404.
[3] S.J. Hurst, E.K. Payne, L. Qin, C.A. Mirkin, Nanostructures 45 (2006) 2672.
[4] S. Kato, H. Shinagawa, H. Okad, G. Kid, K. Mitsuhashi, Sci. Technol. Adv. Mater. 6 (2005) 341.
[5] C.L. Xu, H. Li, G.Y. Zhao, H.L. Li, Matt. Lett. 60 (2006) 2335.
[6] J.H. Jeong, S.H. Kim, Y. Choi, S.S. Kim, Phys. Status Solidi (c) 4 (12) (2007) 4429.
[7] N.V. Hoang, S. Kumar, Gil-Ho Kim, Nanotechnology 20 (2009) 125607.
[8] Y. Liang, L. Zhai, X. Zhao, D. Xu, J. Phys. Chem. B. 109 (2005) 7120.
[9] G. Shen, P.C. Chen, Y. Bando, D. Golberg, C. Zhou, Chem. Mater. 20 (21) (2008) 6779;
L. He, W. Zheng, W. Zhou, H. Du, C. Chen, L. Guo, J. Phys. Condens. Matter 19 (2007) 036216.
[10] K. Maaz, A. Mumtaz, S.K. Hasanain, M.F. Bertino, J. Magn. Magn. Mater. 322 (2010) 2199.
[11] S. Ishrat, K. Maaz, C. Rong, S.H. Kim, M.H. Jung, Gil-Ho Kim, Curr. Appl. Phys. 12 (2011) 65–68.
[12] T. Fukui, C. Sakurai, M. Okuyama, J. Mater. Res. 7 (1992) 791.
[13] E.F. Kneller, F.E. Luborsky, J. Appl. Phys. 34 (1963) 656.

[14] O. Iglesias, A. Labarta, Phys. Rev. B 63 (2001) 184416.
[15] X. Battle, M. Garcia del Muro, J. Tejada, H. Pfeiffer, P. Goand, E. Shinn, J. Appl. Phys. 74 (1993) 3333.
[16] F. Bloch, Z. Phys. 61 (1931) 206.
[17] C.R. Alves, R. Aquino, M.H. Sousa, H.R. Rechenberg, G.F. Goya, F.A. Tourinho, J. Depeyrot, J. Metastable Nanocryst. Mater. 20–21 (2004) 694.
[18] K. Mandal, S. Mitra, P. Anil Kumar, Europhys. Lett. 75 (2006) 618.